Cerebral Cortex August 2013;23:1811–1823
doi:10.1093/cercor/bhs159
Advance Access publication June 17, 2012

The LIM Homeodomain Protein Lhx6 Regulates Maturation of Interneurons and Network Excitability in the Mammalian Cortex

Guilherme Neves[1], Mala M. Shah[3], Petros Liodis[1], Angeliki Achimastou[1], Myrto Denaxa[1], Grant Roalfe[2], Abdul Sesay[2], Matthew C. Walker[4] and Vassilis Pachnis[1]

[1]Division of Molecular Neurobiology, [2]Division of Neurophysiology, MRC National Institute for Medical Research, London, UK [3]Department of Pharmacology, The School of Pharmacy, University of London, London, UK and [4]Institute of Neurology, University College London, London, UK

Address correspondence to Vassilis Pachnis, Division of Molecular Neurobiology, MRC National Institute for Medical Research, The Ridgeway, Mill Hill, London NW7 1AA, UK. Email: vpachni@nimr.mrc.ac.uk

Deletion of LIM homeodomain transcription factor-encoding *Lhx6* gene in mice results in defective tangential migration of cortical interneurons and failure of differentiation of the somatostatin (Sst)- and parvalbumin (Pva)-expressing subtypes. Here, we characterize a novel hypomorphic allele of *Lhx6* and demonstrate that reduced activity of this locus leads to widespread differentiation defects in Sst^+ interneurons, but relatively minor and localized changes in Pva^+ interneurons. The reduction in the number of Sst-expressing cells was not associated with a loss of interneurons, because the migration and number of Lhx6-expressing interneurons and expression of characteristic molecular markers, such as calretinin or Neuropeptide Y, were not affected in *Lhx6* hypomorphic mice. Consistent with a selective deficit in the differentiation of Sst^+ interneurons in the CA1 subfield of the hippocampus, we observed reduced expression of metabotropic Glutamate Receptor 1 in the *stratum oriens* and characteristic changes in dendritic inhibition, but normal inhibitory input onto the somatic compartment of CA1 pyramidal cells. Moreover, *Lhx6* hypomorphs show behavioral, histological, and electroencephalographic signs of recurrent seizure activity, starting from early adulthood. These results demonstrate that *Lhx6* plays an important role in the maturation of cortical interneurons and the formation of inhibitory circuits in the mammalian cortex.

Keywords: Lhx6, LIM homeodomain protein, cortical interneurons

Introduction

The normal activity of the cerebral cortex depends on the formation of functional neuronal networks that are composed of excitatory (glutamate producing) pyramidal neurons and inhibitory γ-amino butyric acid-producing (GABAergic) interneurons. Cortical inhibitory interneurons, which represent approximately 20% of the neurons in the mammalian cortex, constitute an extremely heterogeneous cell population composed of several neuronal subtypes with distinct morphological, electrophysiological, and molecular characteristics (Somogyi and Klausberger 2005; Ascoli et al. 2008). In contrast to pyramidal neurons, which are born in the ventricular zone of the pallium, cortical interneurons originate mostly in the medial and caudal ganglionic eminences (MGE and CGE, respectively), 2 regions of the ventral telencephalon that generate distinct subtypes of interneurons (reviewed in Wonders and Anderson 2006; Rudy et al. 2011; Welagen and Anderson 2011). Cortical interneurons derived from the MGE can be identified by the expression of either the Ca^{2+}-binding protein parvalbumin (Pva) or the neuropeptide somatostatin (Sst; Xu et al. 2004; Fogarty et al. 2007; Rudy *et al.* 2011). Pva^+ interneurons include the fast-spiking basket cells that target mainly the somatic compartment of pyramidal neurons, whereas Sst^+ interneurons include the Martinotti cells that target preferentially distal dendrites (Miles et al. 1996; Kawaguchi and Kubota 1997; Maccaferri et al. 2000; Wang et al. 2004; Butt et al. 2005). Defects in the activity of inhibitory networks in the cortex have been associated with the pathogenesis of several neurodevelopmental disorders, including schizophrenia, autism spectrum disorders, and epilepsy (Rossignol 2011; Rubenstein 2011). Dissecting the molecular and genetic mechanisms that regulate the development of distinct subtypes of cortical interneurons is essential for understanding the fundamental processes underlying formation of functional neuronal networks in the cortex and the pathogenesis of neurodevelopmental and cognitive disorders.

Recent studies have identified a cascade of transcription factors that are critical for the development of cortical inhibitory neurons. In particular, the homeodomain (HD) transcription factors Nkx2.1 and Lhx6 are key components of a molecular cascade required for the development of MGE-derived cortical interneurons (Sussel et al. 1999; Liodis et al. 2007; Du et al. 2008). Lhx6, which belongs to the subfamily of LIM-containing HD (LIM HD) transcription factors, is induced in interneuron precursors as they exit the cell cycle and expression is maintained in mature Pva^+ and Sst^+ inhibitory neurons in the cortex (Liodis et al. 2007). Deletion of *Lhx6* in mice results in delayed tangential migration and abnormal distribution of MGE-derived interneurons in the cerebral cortex (Liodis et al. 2007; Zhao et al. 2008). Moreover, in the cortex of Lhx6-deficient mice, the number of Sst- and Pva-expressing interneurons is severely reduced, but the total number of $GABA^+$ neurons remains largely unaffected (Liodis et al. 2007; Zhao et al. 2008). Although the requirement of Lhx6 for the differentiation of Sst^+ and Pva^+ interneurons has been clearly established, it is currently unclear whether failure of Sst and Pva expression in *Lhx6* mutants is secondary to the migratory deficit and the abnormal allocation of interneuron precursors in cortical layers or results from a cell-intrinsic requirement of Lhx6 for the normal differentiation and maturation of MGE-derived interneurons (Alifragis et al. 2004; Liodis et al. 2007; Zhao et al. 2008). Here, we characterize a novel hypomorphic allele of *Lhx6* ($Lhx6^{LacZ}$), which is associated with a reduced activity of the locus. We show that a single copy of $Lhx6^{LacZ}$ fully rescues the interneuron migration and the perisomatic synaptic inhibition defects that are associated with the *Lhx6* null mutation. However, *Lhx6* hypomorphic animals show a selective deficit in the differentiation of subsets

of interneurons, alterations in dendritic inhibition, and a high propensity to develop spontaneous seizures. Our experiments highlight the complex role(s) of *Lhx6* in the differentiation and maturation of distinct subclasses of cortical interneurons and provide insight into the formation of inhibitory cortical circuits and the pathogenesis of epilepsy.

Materials and Methods

Animals

The generation of the $Lhx6^{-}$ allele has been described previously (Liodis et al. 2007). The $Lhx6^{LacZ}$ allele was propagated in the heterozygous state by backcrossing to C57BL/6 inbred animals, while the $Lhx6^{-}$ null allele was maintained in either the C57BL/6 or the 129S8 background. The homozygous $Lhx6^{-}$ mice analyzed here were F1 (C57BL/6X129S8). $Lhx6^{LacZ/-}$ animals were generated by crossing $Lhx6^{LacZ}$ homozygotes (C57BL/6) with $Lhx6^{-}$ heterozygous animals (129S8). Whenever possible, comparisons between different genotypes were performed using littermates. Details of the genotyping of all mutant mice are available upon request.

For timed pregnancies, the day of vaginal plug detection was considered E0.5. For post-natal animals, the day of birth was considered P0. Animal work was regulated by a UK Home Office Project Licence and approved by the local ethics committee.

Histology and Marker-Expression Analysis

For immunostaining, post-natal animals of either sex were transcardially perfused with 20 mL of 0.9% NaCl followed by 20 mL of 4% paraformaldehyde (PFA) solution in 0.1 M phosphate buffer. Dissected brains were post-fixed overnight in 4% PFA, cryoprotected in 30% sucrose, and either embedded in gelatin and sectioned at 12–20 µm or embedded in agarose and sectioned in a vibratome at 50 µm. Vibratome sections were permeabilized in 0.5% Triton X-100 in phosphate buffered saline (PBS), washed in 0.1% Triton X-100 in PBS (PBT), treated with 10% MetOH, 10% H_2O_2 in PBT to inactivate endogenous peroxidase activity, and washed in PBT. After blocking in 10% fetal calf serum (FCS), 1% bovine serum albumin (BSA) in PBT, sections were incubated with primary antibodies in 1% FCS, 0.1% BSA in PBT (antibody solution) followed by secondary antibody. Peroxidase activity was revealed using 3,3′-diaminobenzidine.

Embryonic tissue was fixed overnight in 4% PFA, cryoprotected, and sectioned at 14 µm. Cryosections were processed as above, with the following modifications. Permeabilization and peroxidase inactivation steps were omitted, blocking and antibody solutions contained 1% BSA and 0.15% glycine in PBT, and secondary antibodies were conjugated with fluorophores. The following antibodies were used: rabbit anti-Lhx6 (1:1000) (Lavdas et al. 1999), mouse anti-Pva (1:1000; Chemicon), rat anti-Sst (1:500; Chemicon), rabbit anti-calretinin (Cr) (1:1000; Chemicon), rabbit anti-Neuropeptide Y (NPY) (1:1000; Peninsula Labs), rabbit anti-mGluR1α (1:500; Immunostar), and mouse anti-β-galactosidase (β-gal) (1:1000; Promega). Secondary antibodies used are as follows: AlexaFluor488-conjugated goat anti-mouse and anti-rabbit and AlexaFluor568-conjugated goat anti-mouse and anti-rabbit (all from Invitrogen; all 1:500).

Proliferation assays were performed by injecting intraperitoneally 5-ethynyl-2′-deoxyuridine (EdU) (30 mg/kg body weight) 2 h prior to perfusion, and revealed using the Click-iT EdU system (Invitrogen) according to the manufacturer's instructions. Nonradioactive *in situ* hybridization on fixed cryostat sections (for embryos) or vibratome sections (for post-natal brains) was performed as described previously (Schaeren-Wiemers and Gerfin-Moser 1993). Riboprobes used were specific for Sst (Liodis et al. 2007) and vasoactive intestinal peptide (VIP) (derived from IMAGE clone 4988915).

Quantification of Images

EdU^{+} nuclei were counted in four to eight 20-µm coronal sections per animal (8–16 hippocampi; bregma levels between −1.34 and −2.80 mm). We counted EdU^{+} nuclei in the entire granule cell layer of the dentate gyrus (DG; superior and inferior blades), and extending approximately 2–3 cell layer widths deep into the hilus (sub-granular zone) where most of the EdU^{+} nuclei were located.

The number of $\beta\text{-gal}^{+}$ and Pva^{+} cells was evaluated using immunohistochemistry (IHC), while the number of Sst^{+} and VIP^{+} cells was evaluated using *in situ* hybridization in vibratome sections (50 µm) of adult (P30) brain. Cells were counted in the primary somatosensory (barrel field) region of the cortex (Paxinos and Franklin 2001) in a defined area (1000 µm width) spanning the pial–white matter extent of the cortex. Radial cell distribution was determined by counting $\beta\text{-gal}^{+}$ cells in 10 equal-sized horizontal bins (bin 1 closer to the white matter). Data are given for each bin as a fraction of the total $\beta\text{-gal}^{+}$ population.

Immunofluorescence (IF) for $\beta\text{-gal}^{+}$, Pva^{+}, and Sst^{+} in the hippocampus (bregma levels −1.34 to −2.80 mm) was quantified using coronal cryosections (20 µm thick) from 4-week–old animals. Double IF for Cr and Sst was quantified in the primary somatosensory cortex (barrel field; bregma between −1.22 and −1.70 mm), while double IF for NPY and Sst was quantified in the hylus region of the DG (bregma levels between −1.34 and −2.80 mm) using coronal cryosections (20 µm thick) from 4-week–old animals. Separate images for each channel were acquired using a confocal microscope (×20 magnification). Markers were initially assessed independently, and were later combined to assess co-localization using the ImageJ software. Cortical layers and hippocampal regions were determined using 4′,6-diamidino-2-phenylindole (DAPI) staining.

The number of $\beta\text{-gal}^{+}$ and Sst^{+} cells in embryonic E13.5 and E17.5 cortices was evaluated in the area between the ventro-pallial boundary and the beginning of the hippocampus, using cryosections (14 µm). All cell counts were performed for at least 3 $Lhx6^{LacZ/+}$ and 3 $Lhx6^{LacZ/-}$ animals, and scored by an observer blind to genotype. Cell numbers for the hippocampus were expressed as positive cells per hippocampal section. Cell numbers for the somatosensory cortex and embryonic pallium were divided by the total surface area analyzed (measured using ImageJ) and normalized to the average density found in $Lhx6^{LacZ/+}$ animals. For layer distribution analysis (Fig. 4P), data are given for each layer as a fraction of the total Sst^{+} population.

Quantification of Gene Expression

RNA was extracted from the forebrain of adult animals of either sex (between P60 and P70) using Trizol (Invitrogen) followed by purification with the RNeasy mini kit (QIAGEN) according to the manufacturer's instructions. Taqman gene expression assays (Applied Biosystems) were performed on cDNA produced with High Capacity RNA-to-cDNA Master Mix (Applied Biosystems) using 1 µM total RNA as a template. The expression levels for each sample were normalized to the expression level of the beta Actin gene. The data were plotted as means of at least 3 animals per genotype and the results were normalized to the average expression level of control animals. Results were confirmed by at least 2 independent cDNA synthesis and TaqMan gene expression assays from each animal.

Electrophysiology

Inhibitory Post-Synaptic Current (IPSC) Recordings from Dentate Granule Cells of 2–3-Week–Old Animals

Acute hippocampal slices were prepared from $Lhx6^{+/-}$, $Lhx6^{-/-}$, $Lhx6^{LacZ/+}$, and $Lhx6^{LacZ/-}$ mice of either sex as described previously (Oren et al. 2009). Briefly, mice were decapitated and the brain was rapidly removed and placed in ice-cold sucrose solution containing: 75 mM sucrose, 87 mM NaCl, 2.5 mM KCl, 0.5 mM $CaCl_2$, 7 mM $MgCl_2$, 1.0 mM NaH_2PO_4, 25 mM $NaHCO_3$, and 25 mM glucose. All $NaHCO_3$ containing solutions were continuously bubbled with 95% O_2/5% CO_2 to maintain a stable pH. Transverse hippocampal slices (300 µm thickness) were cut using a vibrating microtome (Campden Instruments). Slices were kept submerged at 32°C in the sucrose solution for 30–40 min before being transferred to an interface chamber in which they were maintained in Earle's balanced salt solution (Invitrogen) with 3 mM Mg^{2+} and 1 mM Ca^{2+} at room temperature. A single slice was transferred to a submerged recording chamber continuously perfused (2 mL/min) with heated recording artificial cerebrospinal fluid (ACSF) consisting of 119 mM NaCl, 2.5 mM KCl, 1 mM

NaH_2PO_4, 1.3 mM $MgSO_4$, 2 mM 6 $NaHCO_3$, 2.5 mM $CaCl_2$, and 11 mM glucose (295 mOsm). Temperature in the chamber was maintained at 32°C. Whole-cell voltage-clamp recordings were obtained from visually identified granule cells using an infrared differential interference contrast video microscopy system. Patch electrodes (3–7 MΩ) were pulled from borosilicate glass capillary tubing (World Precision Instruments). The intracellular patch pipette solution contained 118 mM Cs-gluconate, 10 mM 4-(2-hydroxyethyl)-1-piperazineethanesulfonic acid (HEPES), 11 mM ethylene glycol-bis(2-aminoethylether)-N,N,N',N'-tetraacetic acid (EGTA), 11 mM $CsCl_2$, 1 mM $MgCl_2$, 3 mM QX314, 2 mM Na_2-adenosine-5′-triphosphate (ATP), and 0.5 mM Na_2-guanosine-5'-triphosphate (GTP), pH 7.25 (285–290 mOsm). To isolate GABAergic currents, slices were perfused with ACSF containing 20 µM 6-ciano-7-dinitroquinoxaline-2,3-dione (CNQX) and 50 µM D-(–)-2-amino-5-phosphonovaleric acid (AP-5), and recordings were done at a holding potential of 0 mV. 25 µM AlexaFluor594 was added to the solution to confirm granule cell morphology after recording.

Whole-cell voltage-clamp data were acquired using an Axopatch 200B amplifier (Molecular Devices, United Kingdom), filtered at 1 kHz and digitized at 10 kHz, using the AxoGraph X software (Axograph Scientific) running on a PowerMac G5 (Apple). Whole-cell access resistance was carefully monitored throughout the recording, and cells were rejected if values changed by >20% (or exceeded 20 MΩ). Spontaneous IPSCs (sIPSCs) were extracted using the automatic event detection algorithm from the Axograph X software. Each captured event was than visually assessed based on rise time, amplitude, and decay properties. Between 100 and 200, individual events were analyzed for each cell. Rise-time histograms were calculated with compiled results from at least 8 cells per genotype (100 events per cell) using the Igor Pro software (Wavemetrics).

IPSC Recordings from Adult Hippocampal CA1 Neurons

Entorhinal–hippocampal slices were obtained from 6- to 9-week–old $Lhx6^{LacZ/+}$ and $Lhx6^{LacZ/-}$ mice of either sex as described previously (Huang et al. 2009). Briefly, mice were intracardially perfused with ice-cold solution containing: 110 mM choline chloride, 2.5 mM KCl, 1.25 mM NaH_2PO_4, 25 mM $NaHCO_3$, 0.5 mM $CaCl_2$, 7 mM $MgCl_2$, and 10 mM dextrose. The brain was then removed and 350-µm–thick hippocampal–entorhinal slices were prepared using a vibratome (Leica VT 1200S). The slices were incubated in a holding chamber at 36°C for 10–15 min followed by 1 h at room temperature. The holding chamber contained external recording solution of the following composition: 125 mM NaCl, 2.5 mM KCl, 1.25 mM NaH_2PO_4, 25 mM $NaHCO_3$, 2 mM $CaCl_2$, 2 mM $MgCl_2$, 10 mM glucose, supplemented with CNQX, and AP-5. 1 µM tetrodotoxin was added to the solution for recording of miniature IPSCs (mIPSCs). Whole-cell voltage-clamp recordings (holding potential −70 mV) were obtained from the soma and apical dendrites (approximately 200 µm from the soma) of CA1 hippocampal pyramidal neurons. The internal recording pipette solution contained: 140 mM KCl, 10 mM HEPES, 2 mM $MgCl_2$, 0.2 mM EGTA, 4 mM Na_2-ATP, 0.3 mM Tris-GTP, 14 mM Tris-phosphocreatine; pH was adjusted to 7.3 with KOH. Pipettes containing any of these internal solutions had resistances of 5–12 MΩ. Series resistance was usually in the order of 10–30 MΩ and was approximately 70% compensated. Data were acquired using pClamp 8.2 (Molecular Devices). All experiments were done at near physiological temperatures (i.e. 34–36°C). IPSC recordings were analyzed using Mini-analysis program (v6.07, Synaptosoft). Decay times and amplitudes of events were obtained by fitting the averaged EPSC or IPSC with a single exponential equation $I(t) = A \exp(-t/\tau)$, where I is the current amplitude at any given time (t), A peak amplitude of IPSC, and τ decay time constant. Unless otherwise specified, all data are presented as mean ± standard error of the mean (SEM) and statistical significance was determined using unpaired Student's t-test. Statistical significance of $P < 0.05$ is indicated as asterisk in all figures.

Chronic Electroencephalographic Recording

Adult $Lhx6^{LacZ/+}$ and $Lhx6^{LacZ/-}$ littermate mice of either sex (aged 3–8 months) were implanted with electrodes for chronic recordings. For this, mice were anesthetized with isofluorane (2–3% [v/v]; Abbot) using a flow-through vaporizer (VetTeach) and were positioned in a stereotaxic frame. Teflon-coated nickel/chromium wire electrodes (0.025-mm diameter; Advent) soldered to a miniature connector, or polyimide-coated stainless steel electrode (0.23-mm diameter) assemblies (PlasticsOne Inc., VA, USA), were surgically implanted into the hippocampal area using the following stereotaxic co-ordinates (in mm): 1.5–2.0 lateral to midline, 2.0–2.5 posterior to bregma, and 1.2–1.7 below the cortex surface. A Teflon-coated silver wire electrode (0.125-mm diameter) locally positioned below the skin but above the skull, was used as a reference.

All mice were kept on 12 h light–dark cycles. Electroencephalographic (EEG) recordings were obtained 7 days later using a neurolog amplifier and acquired on a PowerMac G5 computer using the NeuroMatic (www.neuromatic.thinkrandom.com) package of extensions for IgoPro. The EEG was band-pass filtered from 0.5 to 250 Hz and sampled at 500 Hz. Recordings were performed on freely moving mice in the test cage, at random times in 1–3-h recording periods using both light and dark conditions, during a total period of 10–60 days. All recordings were done during the light phase of the light–dark cycle. Throughout the recording period an observer was present, and scored seizure behavior using the scale described in Monory et al. (2006). Periods of artifact due to movement, eating, or grooming were removed from the analysis. Electrographic seizure activity was defined as the appearance of high amplitude (>3 times baseline activity), rhythmic fast activity in the beta-gamma range (15–40 Hz; de Curtis and Gnatkovsky 2009) that lasted a minimum of 90 s.

Susceptibility to Kainic Acid-Induced Seizures

Kainic acid (19 mg/kg body weight diluted in 0.9% NaCl; Tocris Ltd.) was administered to adult males (5–7 months old) $Lhx6^{LacZ/+}$, $Lhx6^{LacZ/-}$, and $Lhx6^{+/+}$ mice by intraperitoneal injection. Mice were placed in a test cage in a darkened room and seizures were monitored by an observer blind to the genotype of the mice for 90 min after the injection and scored in 10 min intervals according to the scale defined in Monory et al. (2006). Videos were recorded during the scoring period and the accuracy of scoring was assessed by inspection of the videos.

Results

$Lhx6^{LacZ}$ Rescues the Post-natal Lethality of Lhx6 Null Mutants

To dissect the role of the LIM HD transcription factor Lhx6 on cortical interneuron development, we examined the phenotypic effects of $Lhx6^{LacZ}$, a novel allele generated fortuitously during our efforts to target the *Lhx6* locus in ebryonic stem cells (Liodis et al. 2007). In the case of $Lhx6^{LacZ}$, the entire targeting construct was inserted into the 3′ region of *Lhx6* without disrupting its coding sequences but bringing the *LacZ* reporter under the control of the regulatory regions of the locus (Fig. 1*A* and data not shown). In contrast to *Lhx6* null mutants (Liodis et al. 2007), compound heterozygous $Lhx6^{LacZ/-}$ and homozygous $Lhx6^{LacZ/LacZ}$ animals survived to adulthood, were fertile and showed no gross morphological abnormalities, indicating that $Lhx6^{LacZ}$ rescues the post-natal lethality of Lhx6-deficient mice. Consistent with these observations, in $Lhx6^{LacZ/-}$ animals all β-gal-expressing (MGE-derived) cortical interneurons were also positive for Lhx6, as assessed by immunostaining with a polyclonal antibody raised against this protein (Fig. 1*B*, Liodis et al. 2007). However, quantification of Lhx6 transcripts in the forebrain of animals with different combinations of wild type, null ($Lhx6^{-}$), and $Lhx6^{LacZ}$ alleles, showed that $Lhx6^{LacZ}$ generates approximately 40% of the mRNA produced by the wild-type locus (Fig. 1*C*). Detailed mapping of cDNA generated from the $Lhx6^{LacZ}$ allele suggested that insertion of the targeting vector did not affect the splicing pattern of the primary Lhx6

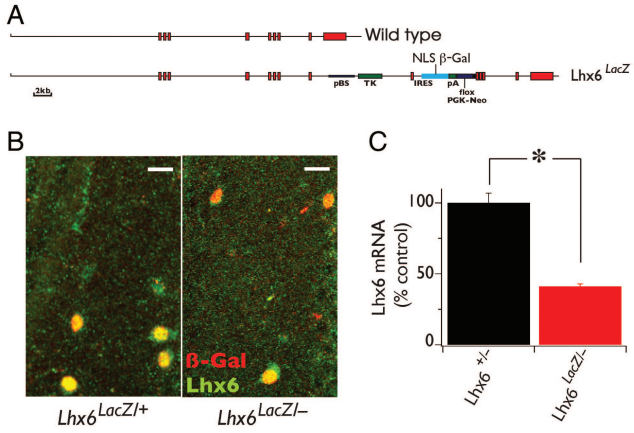

Figure 1. *Lhx6*^{LacZ} is a novel hypomorphic allele of the *Lhx6* locus. (*A*) Genomic organization of the wild type (top) and the *Lhx6*^{LacZ} (bottom) alleles of *Lhx6*. Exons are represented by red boxes. (*B*) Double-IF staining of hippocampal CA1 *stratum oriens* from *Lhx6*$^{LacZ/+}$ and *Lhx6*$^{LacZ/-}$ animals using antibodies specific for Lhx6 (green) and β-gal (red). (*C*) The transcriptional activity of the wild type and *Lhx6*^{LacZ} alleles was compared (in the background of the null allele) using quantitative real-time polymerase chain reaction with cDNA generated from the forebrain of adult *Lhx6*$^{+/-}$ and *Lhx6*$^{LacZ/-}$ animals (P60) as template and TaqMan probes for Lhx6 mRNA. Error bars show SEM. *$P < 0.05$. $n = 3$ animals per genotype. Scale bars 20 μm.

transcript (data not shown). Taken together, these findings suggest that *Lhx6*^{LacZ} represents a novel hypomorphic allele of the murine *Lhx6* locus that is capable of rescuing the early post-natal lethality of *Lhx6* null mutants.

Normal Migration of MGE-Derived Cortical Interneurons in Lhx6^{LacZ} *Hypomorphic Mice*

Lhx6-deficient mice are characterized by delayed tangential migration and abnormal distribution of MGE-derived cortical interneurons in the neocortex and the hippocampus (Alifragis et al. 2004; Liodis et al. 2007; Zhao et al. 2008). To examine whether the residual activity of *Lhx6*^{LacZ} is sufficient to support normal tangential migration of cortical interneuron precursors, we used the β-gal reporter to follow these cells in the forebrain of *Lhx6*$^{LacZ/-}$ animals (hereafter referred to as *Lhx6* hypomorphs). No difference in the position of β-gal$^+$ cells was detected between hypomorphic and *Lhx6*$^{LacZ/+}$ (control) embryos at E13.5 (Fig. 2*A*,*B*). Moreover, we detected no difference in the number and distribution of β-gal$^+$ cells in the somatosensory cortex or the hippocampus of 4-week–old control and hypomorphic animals (Fig. 2*C*–*F*). These observations were further confirmed by quantifying the density of β-gal$^+$ cells in the pallium of E13.5 and 17.5 embryos, the somatosensory cortex of post-natal day (P)8 mice or the

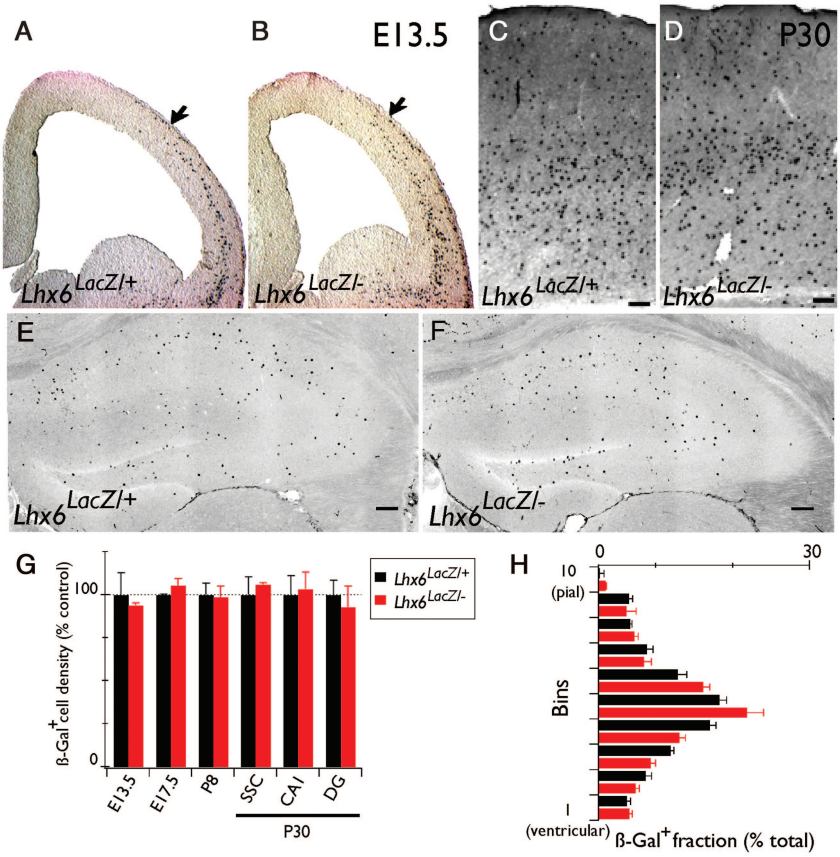

Figure 2. Normal number and distribution of cortical interneurons in *Lhx6*$^{LacZ/-}$ animals. (*A* and *B*) X-Gal staining of coronal brain sections from E13.5 *Lhx6*$^{LacZ/+}$ and *Lhx6*$^{LacZ/-}$ embryos. Coronal brain sections from *Lhx6*$^{LacZ/+}$ and *Lhx6*$^{LacZ/-}$ animals processed for IHC (neocortex, *C* and *D*) or IF (hippocampus, *E* and *F*) with a β-gal–specific antibody. (*G*) Average density of β-gal$^+$ cells in the pallium (for embryos) or the somatosensory cortex (for P8 and P30) and the CA1 and DG areas of the hippocampus of *Lhx6*$^{LacZ/+}$ and *Lhx6*$^{LacZ/-}$ animals at the indicated developmental stages. (*H*) Quantification of the radial distribution of β-gal$^+$ cells in the somatosensory cortex. $n = 3$ animals were analyzed per genotype, area, and developmental stage. Scale bars = 100 μm.

somatosensory cortex and the hippocampus (CA1 and DG) of P30 animals from the 2 genotypes (Fig. 2*G*). Finally, no difference was observed in the distribution of β-gal^{+} cells along the pial-ventricular axis of the somatosensory cortex of control and hypomorphic mice (Fig. 2*H*). Together, these findings demonstrate that a single copy of *Lhx6*^{LacZ} supports the development of a normal complement of MGE-derived cortical interneurons, highlighted by normal tangential migration and distribution into cortical layers.

Deficits of Cortical Inhibitory Circuits in Lhx6 Null Mutants are Rescued by the Lhx6^{LacZ} *Hypomorphic Allele*

To examine whether *Lhx6*^{LacZ} is capable of supporting the formation of functional inhibitory circuits in the cortex, we first analyzed the activity of cortical interneurons in Lhx6-deficient animals. For this, we recorded sIPSCs from DG granule cells in acute hippocampal slices of 2–3-week–old *Lhx6*$^{+/-}$ and *Lhx6*$^{-/-}$ mice. As shown in Figure 3 (*A*–*C*), we observed a striking reduction in the frequency of sIPSCs

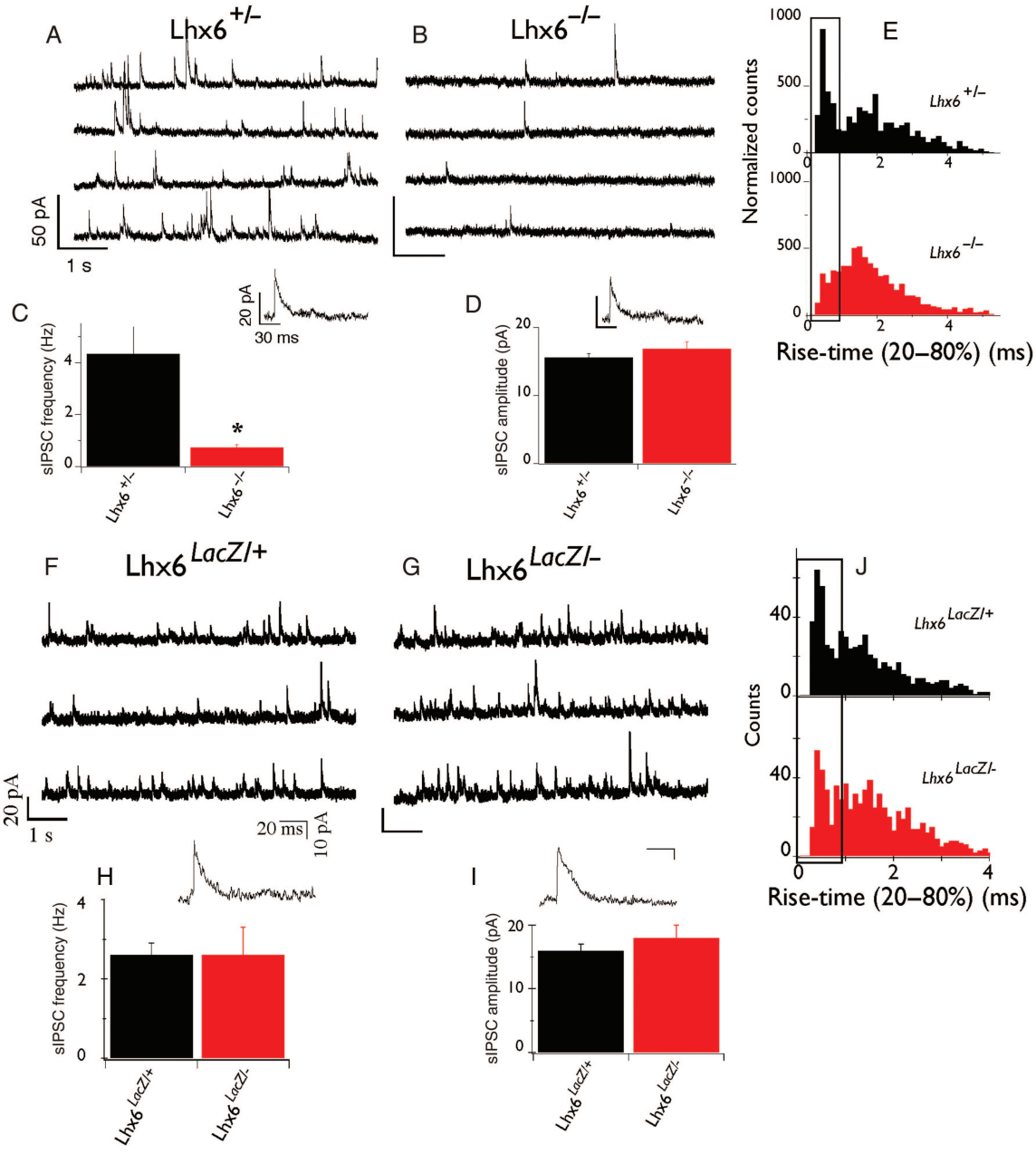

Figure 3. *Lhx6* null but not hypomorphic animals have severe reduction in inhibitory synaptic currents. (*A* and *B*) Representative voltage-clamp recordings from DG granule cells of control (*Lhx6*$^{+/-}$; *A*) and *Lhx6*$^{-/-}$ (*B*) slices. Individual IPSCs with increased temporal resolution are also shown. Units at scale bars in *A* and *B* are the same. (*C*) Average frequency of sIPSCs and (*D*) average amplitude of sIPSCs from control and mutant slices. (*E*) Normalized histogram of sIPSC rise time (20–80%) from control (black) and mutant (red) slices. Boxed area indicates events with rapid kinetics. *$P < 0.05$. $n = 12$ cells (6 animals) control and 21 cells (8 animals) mutants. In contrast to Lhx6-deficient animals, normal sIPSCs were recorded from the somatic compartment of DG granule cells from *Lhx6*$^{LacZ/-}$ animals. (*F* and *G*) Representative voltage-clamp recordings from DG granule cells from control (*F*) and *Lhx6*$^{LacZ/-}$ (*G*) slices. Individual IPSCs with increased temporal resolution are also shown. Units of scale bars in *F* and *G* are the same. Average frequency (*H*) and amplitude (*I*) of sIPSCs from control and *Lhx6*$^{LacZ/-}$ animals. (*J*) Histograms of sIPSC rise times from control (top) and *Lhx6*$^{LacZ/-}$ (bottom) animals show no major difference between control (black) and mutant (red) slices. $n = 18$ cells (from 9 *Lhx6*$^{LacZ/+}$ animals) and 27 cells (from 11 *Lhx6*$^{LacZ/-}$ mutants).

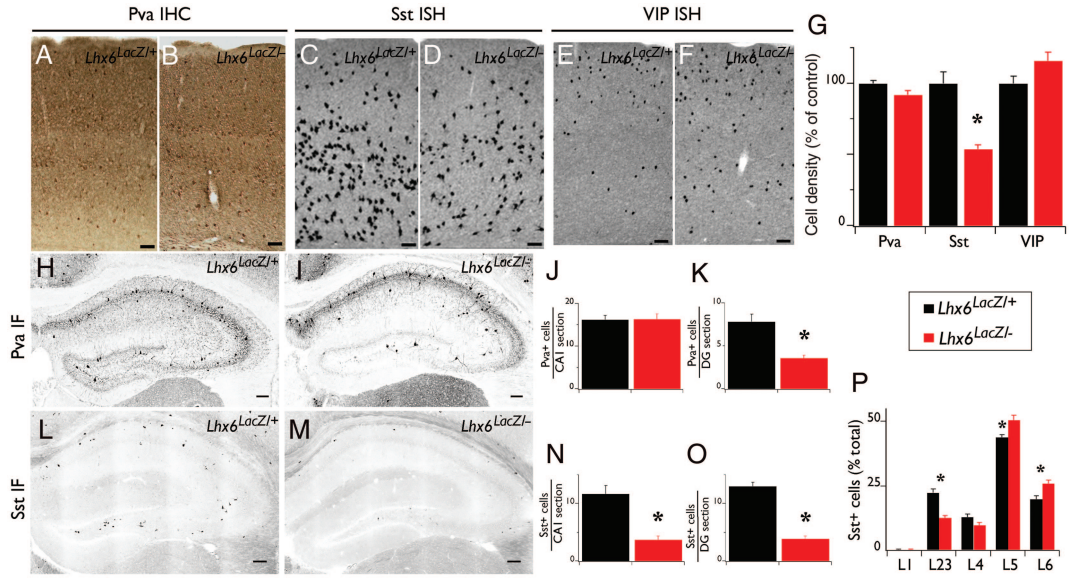

Figure 4. Differentiation defects of cortical interneurons in *Lhx6* hypomorphic animals. IHC of coronal brain sections from control ($Lhx6^{LacZ/+}$; *A*) and *Lhx6* hypomorphic ($Lhx6^{LacZ/-}$; *B*) animals with antibodies specific for Pva. *In situ* hybridization of coronal brain sections from control (*C* and *E*) and *Lhx6* hypomorphic (*D* and *F*) animals with a Sst (*C* and *D*) or a vasoactive intestinal peptide (VIP) riboprobe (*E* and *F*). (*G*) Quantification of the density of interneurons expressing the indicated markers from the somatosensory cortex of *Lhx6* hypomorphic animals (red bars) relative to their control littermates (black bars); $n = 3$ animals per genotype. IF in the hippocampus of control (*H* and *L*) and of *Lhx6* hypomorphic (*I* and *M*) animals with antibodies specific for Pva (*H* and *I*) or Sst (*L* and *M*). (*J, K, N, O*) Quantification of IF experiments; $n = 5$ animals per genotype. (*P*) An increased proportion of the Sst^+ cells are located in the deeper layers of the neocortex of *Lhx6* hypomorphs; $n = 7$ animals per genotype. All significant differences ($P < 0.05$) are indicated above the graphs with an asterisk. Scale bars 100 μm.

recorded in slices from homozygous *Lhx6* null animals (0.7 ± 0.1 Hz, $n = 21$) relative to heterozygous littermates (4.3 ± 1.0 Hz, $n = 12$; $P = 0.02$), indicating that Lhx6 activity is required for the formation of functional inhibitory synapses on DG granule cells. Despite the reduced frequency, no significant difference in sIPSC amplitude was observed between the 2 genotypes (heterozygous: 15.6 ± 0.6 pA, $n = 12$ and nulls: 17.0 ± 1.0 pA, $n = 21$; $P = 0.3$; Fig. 3*D*), suggesting that the post-synaptic function of GABA receptors and transporters remains unaffected in *Lhx6* null mutants. However, analysis of the rise-time kinetics of individual sIPSCs revealed a preferential reduction in mutant slices of events with rapid rise time (boxed in Fig. 3*E*), which is likely to correspond to sIPSCs generated in the perisomatic compartment (Miles et al. 1996; Maccaferri et al. 2000). Thus, 36% of sIPSCs in heterozygous slices have rise times <1 ms compared with 26% in the nulls. This observation is consistent with the decreased number of Pva^+ cortical interneurons in $Lhx6^{-/-}$ mice, a major subset of which (basket cells) preferentially targets the perisomatic region of glutamatergic neurons (Miles et al. 1996; Kawaguchi and Kubota 1997; Butt et al. 2005).

In contrast to Lhx6-deficient mice, no significant difference was observed in either the frequency or the amplitude of sIPSCs recorded from DG granule cells in slices from *Lhx6* hypomorphic and control animals (frequency of sIPSCs in controls was 2.6 ± 0.3 Hz, $n = 11$ and in hypomorphs 2.6 ± 0.7 Hz, $n = 27$; $P = 0.9$; Fig. 3*F–J*). In addition, the sIPCS rise times were no different between the 2 genotypes (41% of sIPSCs was fast in controls relative to 43% in hypomorphs; boxed region in Fig. 3*J*). These electrophysiological studies demonstrate that *Lhx6* activity is necessary for the formation of functional inhibitory networks in the mammalian cortex and that the hypomorphic $Lhx6^{LacZ}$ allele is capable of rescuing the dramatic inhibitory deficits identified in Lhx6-deficient animals.

Lhx6 Hypomorphic Mice Show Partial- and Region-Specific Deficits in the Differentiation of MGE-Derived Cortical Interneurons

In Lhx6-deficient animals, the expression of characteristic markers of mature cortical interneurons born in the MGE, such as Sst and Pva, are virtually absent (Liodis et al. 2007; Zhao et al. 2008). However, it is currently unclear whether the failure of Sst and Pva induction indicates a direct requirement of Lhx6 for the differentiation and maturation of cortical interneurons or instead reflects the delayed migration and abnormal distribution of these cells in the pallium. To explore this issue, we analyzed the differentiation of cortical interneurons in 4-week–old hypomorphic mice, which are characterized by reduced activity of *Lhx6* but normal migration and distribution of cortical interneurons. In contrast to *Lhx6* null mutants, the density of Pva^+ interneurons in the somatosensory cortex of Lhx6 hypomorphs was similar to that in control mice (92 ± 3%, $n = 3$, $P = 0.1$; Fig. 4*A,B,G*). In addition, no reduction in the number of Pva^+ interneurons was observed in the CA1 region of the hippocampus in *Lhx6* hypomorphs relative to controls (16.2 ± 1.0 cells/section in hypomorphs vs. 16.3 ± 1.3 cells/section in controls; $n = 5$, $P = 0.9$; Fig. 4*H–J*). However, fewer Pva^+ cells were observed in the DG of hypomorphic hippocampi (3.6 ± 0.3 cells/section) relative to controls (7.8 ± 0.9 cells/section; $n = 5$, $P < 0.01$; Fig. 4*H,I,K*). These findings indicate that the $Lhx6^{LacZ}$ allele is generally capable of supporting normal differentiation of Pva^+ cortical interneurons. Nevertheless, a DG-specific differentiation defect of Pva^+ interneurons was observed in *Lhx6* hypomorphic mice.

In contrast to the Pva^+ cortical interneurons, we found a widespread deficit in the differentiation of Sst^+ interneurons in the cortex of *Lhx6* hypomorphic animals. Thus, the density of Sst^+ interneurons in the somatosensory cortex of

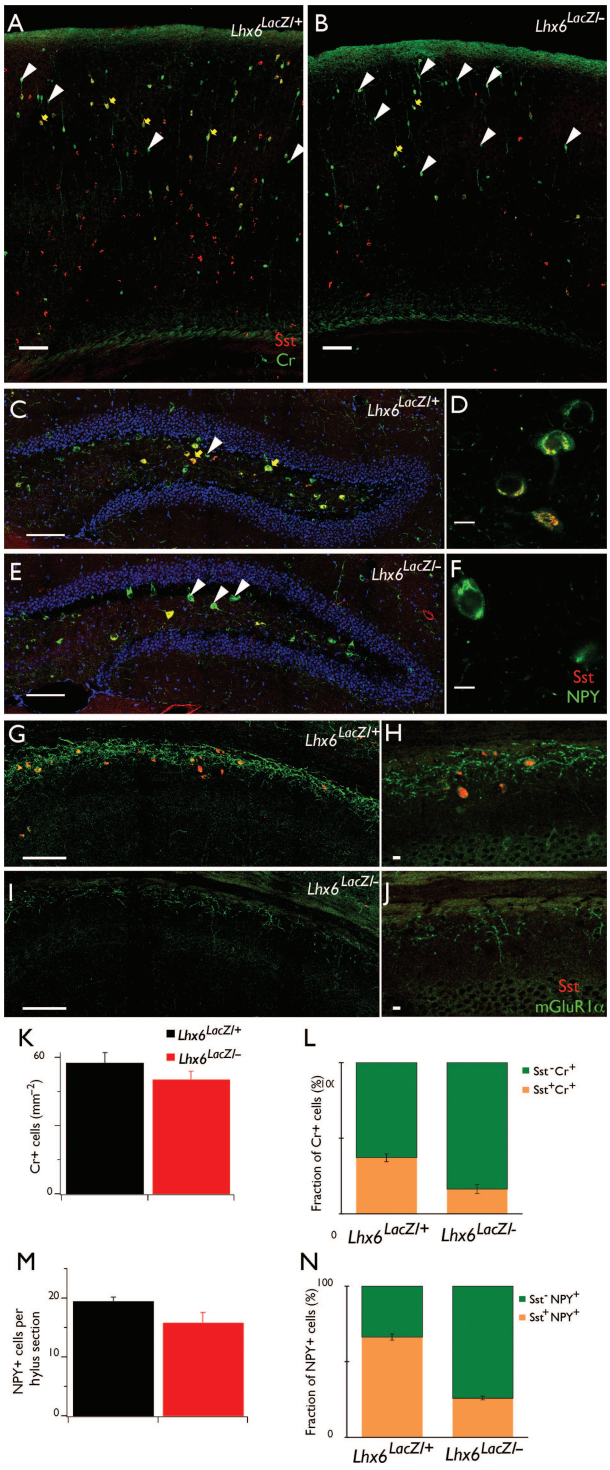

Figure 5. Partial differentiation of Sst^+ interneurons in *Lhx6* hypomorphic animals. Double IF of coronal brain sections from control (*A*) and *Lhx6* hypomorphic (*B*) animals with antibodies specific for Cr (green) and Sst (red). No changes were observed in the total density of Cr^+ cells (*K*), but the fraction of Cr^+ cells that co-express Sst (yellow arrows in *A* and *B*, orange bars in *L*) is significantly reduced in *Lhx6* hypomorphic animals, resulting in an increased fraction of Cr^+Sst^- cells (white arrowheads in *A* and *B*, green bars in *L*). Double IF of the DG hylus region from control (*C*) and *Lhx6* hypomorphic (*E*) animals with antibodies specific for NPY (green) and Sst (red). No changes were observed in the total number of NPY^+ cells (*M*), but the fraction NPY^+Sst^+ cells (yellow arrows in *C* and *E*, orange bars in *N*) is reduced in hypomorphs. (*D* and *F*) show single confocal sections of representative examples of NPY^+Sst^+ (*D*) and NPY^+Sst^- (*F*) cells at higher resolution. Double IF of the *stratum oriens* of the CA1 region of the hippocampus from control (*G*) and *Lhx6* hypomorphic (*I*) animals with antibodies specific for mGluR1α (green) and Sst (red), showing reduced expression of mGluR1α in mutant animals. (*H* and *J*) show single confocal sections at higher resolution. Scale bars 100 μm (*A*, *B*, *C*, *E*, *G*, *I*) and 10 μm (*D*, *F*, *H*, *J*). In (*C*–*F*), cell nuclei are counterstained with 4′,6-diamidino-2-phenylindole (DAPI) (blue), to reveal the granule cell layer.

hypomorphic animals was 57 ± 7% relative to controls ($n = 3$, $P = 0.01$; Fig. 4*C*,*D*,*G*). The Sst^+ interneurons identified in hypomorphic animals were preferentially located in the deeper layers (Fig. 4*P*), suggesting that Sst expression in interneurons that normally colonize the upper cortical layers is dependent on high levels of *Lhx6* activity. Consistent with the observed deficit in the neocortex, the density of Sst^+ interneurons in the CA1 and DG subfields of the hippocampus was also reduced in hypomorphic mice to ~30% of the level observed in control littermates ($n = 5$ for both areas, $P < 0.01$; Fig. 4*L*–*O*). Therefore, despite the normal density of β-gal^+ cells in the cortex of *Lhx6* hypomorphic mice (Fig. 2), which indicates a normal complement of MGE-derived cortical interneurons, these animals are characterized by a widespread deficit in the differentiation of the Sst-expressing subtype of interneurons. Therefore, the $Lhx6^{LacZ}$ allele provides only a partial rescue of the differentiation defects of Sst^+ interneurons observed in *Lhx6* null mutants. Finally, and consistent with the normal differentiation of CGE-derived cortical interneurons in *Lhx6* null mutants, no difference was observed in the VIP-expressing interneurons of the somatosensory cortex of hypomorphic mice (116 ± 6%, $n = 3$, $P = 0.1$; Fig. 4*E*–*G*).

To further characterize the differentiation of MGE-derived cortical interneurons in *Lhx6* hypomorphic animals, we next examined the expression of other molecular markers that are normally co-expressed with Sst: The calcium-binding protein Cr (Xu et al. 2006; Fogarty et al. 2007), the NPY (Fu and van den Pol 2007; Xu, Roby et al. 2010), and the metabotropic Glutamate Receptor subtype mGluR1α (Baude et al. 1993; Mannaioni et al. 2001; Ferraguti et al. 2004; Lapointe et al. 2004). Despite the reduced representation of Sst^+ interneurons, the density of Cr^+ neurons was similar in the 2 genotypes (Fig. 5*A*,*B*,*K*), resulting in an increased proportion of Cr^+Sst^- interneurons in *Lhx6* hypomorphs (84 ± 3%) relative to controls (63 ± 3%; $n = 3$, $P < 0.01$; compare green bars in Fig. 5*L*). In the hylus region of the DG, most NPY^+ interneurons normally co-expressed Sst (Fig. 5*C*,*D*; Fu and van den Pol 2007). In *Lhx6* hypomorphic animals, the number of NPY^+ interneurons was similar to controls (Fig. 5*M*), resulting in a relative increase in the fraction of NPY^+Sst^- interneurons (Fig. 5*E*,*F*,*N*). In contrast, the expression of mGluR1α in the *stratum oriens* of the CA1 and CA3 subfields of the hippocampus was strongly down-regulated (Fig. 5*G*–*J*). These findings suggest that in *Lhx6* hypomorphs, a significant fraction of MGE-derived cortical interneurons selectively lose Sst and mGluR1α expression but maintain expression of other molecular markers such as Cr and NPY. Taken together, these experiments indicate that the reduced activity of *Lhx6* (associated with the hypomorphic $Lhx6^{LacZ}$ allele) is sufficient to maintain a normal complement of MGE-derived cortical interneurons but results in a widespread (albeit partial) defect in the differentiation of Sst^+ cortical interneurons and a DG-specific deficit in the differentiation of Pva^+ interneurons.

Changes of Dendritic Inhibition in the CA1 Region of the Hippocampus of Lhx6 Hypomorphic Animals

Pva$^+$ interneurons synapse primarily onto the cell body and axon initial segment of glutamatergic neurons, but Sst$^+$ interneurons tend to target their dendrites (Miles et al. 1996; Kawaguchi and Kubota 1997; Maccaferri et al. 2000; Butt et al. 2005). The differentiation deficit of Sst$^+$ cortical interneurons, in conjunction with the normal frequency of sIPSCs in dentate granule cells, suggested that Lhx6 hypomorphic animals are characterized by changes in inhibitory synaptic function specifically at dendritic, rather than somatic locations. Since somatic voltage-clamp recordings of synaptic currents elicited at dendritic locations can be impaired by the filtering effects of the dendritic arborization (Segev and Rall 1998; Williams and Mitchell 2008), we tested this hypothesis by directly recording sIPSCs and mIPSCs from the distal dendrites (~200 μm from the soma) close to *stratum lacunosum moleculare* (which receive a major input from Sst$^+$ Oriens Lacunosum Moleculare —OLM cells), as well as the soma of CA1 pyramidal neurons in *stratum pyramidale* (which receives synaptic input mostly from Pva$^+$ basket and axo-axonic cells; Somogyi and Klausberger 2005; Andrasfalvy and Mody 2006). We found no differences in either the frequency or the amplitude of sIPSCs or mIPSCs recorded from CA1 pyramidal cell soma between *Lhx6* hypomorphic and control mice (mIPSC frequency in controls 3.3 ± 0.5 Hz, $n = 15$ and in hypomorphs 2.2 ± 0.6 Hz, $n = 12$; $P = 0.2$; sIPSC frequency in controls and in hypomorphs = 3.2 ± 0.4, $n = 15$ and 3.7 ± 1.4, $n = 12$, respectively; Fig. 6*A–F* and data not shown). These results are consistent with the normal number of Pva$^+$ interneurons in the CA1 region of hypomorphic mice and suggest that the inhibitory input on the soma of pyramidal neurons in *Lhx6* hypomorphs mice is normal. There was also no significant difference in sIPSC frequency (0.88 ± 0.45 Hz, $n = 7$ in controls vs. 1.19 ± 0.66 Hz, $n = 6$ in hypomorphs; $P = 0.8$) or amplitude recorded from control and *Lhx6* hypomorph CA1 dendrites. However, we observed that the frequency of dendritic mIPSCs in *Lhx6* hypomorphs (0.72 ± 0.34 Hz, $n = 6$) was 6-fold higher relative to controls (0.12 ± 0.05 Hz, $n = 7$, $P = 0.04$; Fig. 6*G–I*), suggesting an increased number or higher release probability of inhibitory synapses at the distal dendrites of CA1 pyramidal neurons in these animals. In addition, the decay time constant of mIPSCs in hypomorphic mice (7.7 ± 1.3 ms) was significantly smaller relative to controls (12.3 ± 1.3 ms; $P = 0.01$; Fig. 6*K*,*L*). Together, these experiments reveal characteristic changes in the function of inhibitory synapses at the distal dendrites of glutamatergic neurons in *Lhx6* hypomorphic mice.

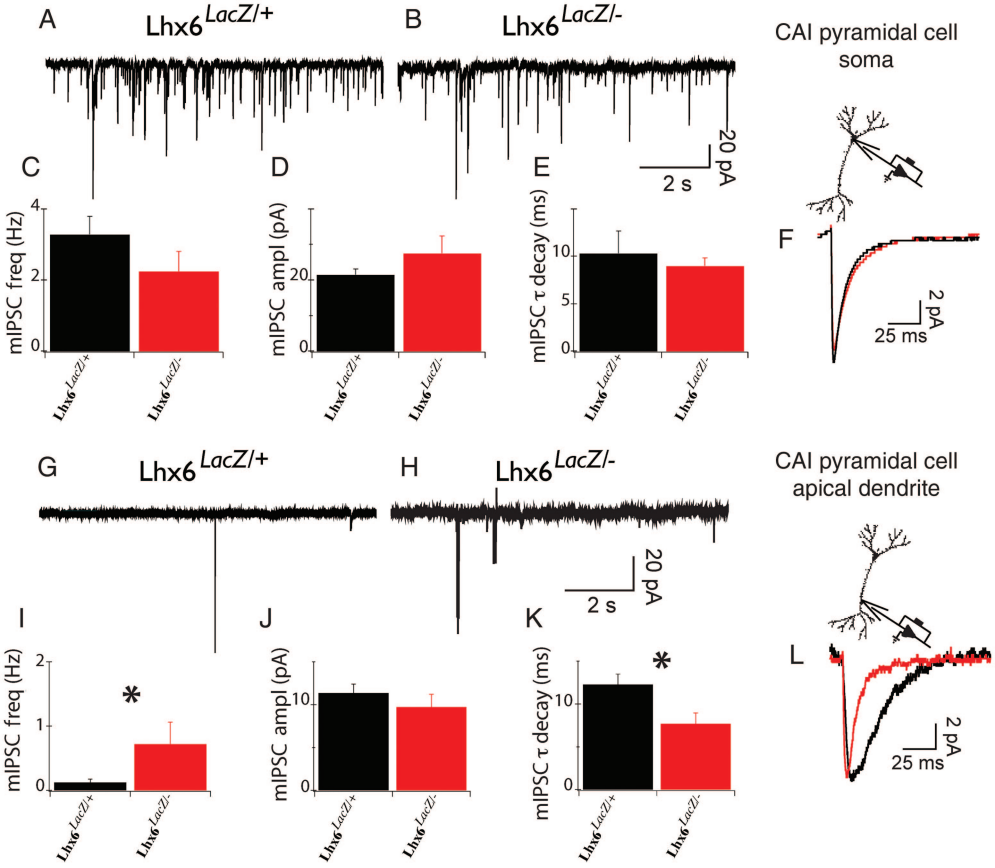

Figure 6. Miniature synaptic currents recorded from dendrites of *Lhx6*$^{LacZ/-}$ animals show specific changes of their properties. (*A* and *B*) Representative mIPSC traces obtained from the soma of *Lhx6*$^{LacZ/+}$ (*A*) and *Lhx6*$^{LacZ/-}$ (*B*) CA1 pyramidal neurons. (*C–E*) Average frequency (*C*), amplitude (*D*), and decay time constants (*E*) of mIPSCs from the soma of 14 *Lhx6*$^{LacZ/+}$ and 12 *Lhx6*$^{LacZ/-}$ neurons. (*F*) Overlay of the average mIPSC obtained from control (*Lhx6*$^{LacZ/+}$; black) and *Lhx6*$^{LacZ/-}$ (red) cells. (*G* and *H*) mIPSC recordings obtained from apical dendrites (200 μm from the soma) of hippocampal CA1 neurons from *Lhx6*$^{LacZ/+}$ (*G*) and *Lhx6*$^{LacZ/-}$ (*H*) animals. (*I–K*) Mean frequency (*I*), amplitude (*J*), and decay (*K*) of mIPSCs from 7 *Lhx6*$^{LacZ/+}$ and 6 *Lhx6*$^{LacZ/-}$ dendrites. *$P < 0.05$. (*L*) Overlay of average dendritic mIPSCs from *Lhx6*$^{LacZ/+}$ (black) and *Lhx6*$^{LacZ/-}$ (red). Note statistically significant changes in the average frequency (*I*) and decay (*K*).

Adult Lhx6 Hypomorphic Mice are Characterized by Spontaneous Tonic-Clonic Seizures

Given the widespread differentiation defect of Sst^+ cortical interneurons and the associated changes in dendritic inhibition observed in *Lhx6* hypomorphic mice, we asked whether these animals develop seizures. To explore this possibility, we first compared the sensitivity of hypomorphic and control animals to convulsants (Monory et al. 2006). *Lhx6* hypomorphs injected with 19 mg/kg kainic acid showed more severe seizures which had faster onset and lasted longer relative to control littermates (Fig. 7*A,B*). Interestingly, no difference was observed between $Lhx6^{LacZ/+}$ and wild-type animals (Fig. 7*A,B*). Mild stress (such as handling and tail suspension) also led to generalized seizures in approximately 70% of hypomorphic mice while under similar conditions no control animals developed seizures (data not shown). Next, we video-recorded the behavior of *Lhx6* hypomorphic mice in their home cage and observed (in 2 of 5 mice) episodes of rearing and loss of postural control, indicative of stage 4 generalized tonic-clonic seizures (according to Monory et al. 2006; Supplementary Movie S1). No seizures were detected in 3 control mice that were video-recorded for a similar length of time. To analyze the seizure phenotype of *Lhx6* hypomorphs further, we implanted electrodes in the hippocampus of 3–8-month–old mice and recorded EEG activity of awake behaving animals over several 1–3-h recording sessions.

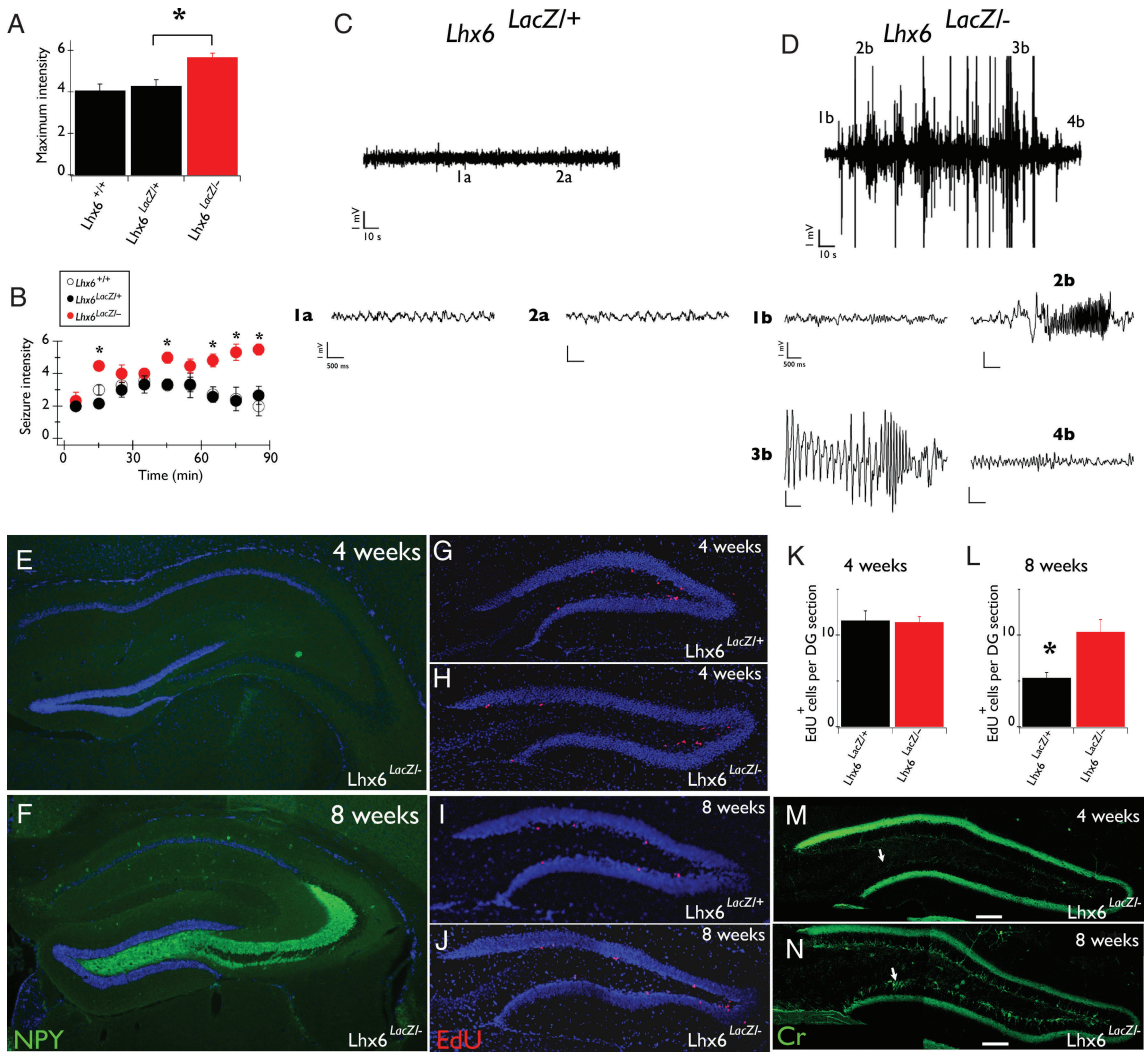

Figure 7. $Lhx6^{LacZ/-}$ animals show spontaneous seizures from early post-natal stages. (*A*) The maximum intensity of convulsions of $Lhx6^{LacZ/-}$ (red bar) and control $Lhx6^{LacZ/+}$ or $Lhx6^{+/+}$ littermates (black bars) upon administration of 19 mg/kg kainic acid. (*B*) Severe convulsions appeared earlier and lasted longer in $Lhx6^{LacZ/-}$ animals (red circles) relative to controls ($Lhx6^{LacZ/+}$, black circles and $Lhx6^{+/+}$, white circles). Asterisks represent statistically significant ($P < 0.01$) differences between $Lhx6^{LacZ/-}$ and control littermates. (*C*) Typical EEG from the hippocampus of a freely moving control ($Lhx6^{LacZ/+}$) animal. (1a and 2a) show increased temporal resolution of the areas indicated in *C*. (*D*) EEG during seizure from a hypomorphic animal ($Lhx6^{LacZ/-}$), demonstrating different seizure stages: 1b—Baseline EEG, 2b—beginning of seizure, 3—late stages of seizure, and 4b—return to baseline after seizure. The same units apply to all scale bars in 1a, 2a, and 1b–4b. (*E* and *F*) NPY IF in the hippocampus of 4-week (*E*) and 8-week–old (*F*) $Lhx6^{LacZ/-}$ animals. Note the intense NPY staining specifically in mossy fibers of 8-week–old animals. (*G–J*) EdU incorporation in the inner margin of the granular cell layer of the DG of 4-week (*G* and *H*) and 8-week–old (*I* and *J*) control ($Lhx6^{LacZ/+}$; *G* and *I*) and hypomorphic ($Lhx6^{LacZ/-}$; *H* and *J*) animals. (*K* and *L*) Quantification of the experiment shown in *G–J* for 4-week (*K*) and 8-week–old (*L*) animals. *$P = 0.01$, $n = 3$ $Lhx6^{LacZ/+}$ animals, or $n = 6$ $Lhx6^{LacZ/-}$ animals. (*M* and *N*) Cr IF in the hippocampus of 4-week (*M*) and 8-week–old (*N*) $Lhx6^{LacZ/-}$ animals. Note that Cr-specific signal is observed in the inner area of the granular cell layer (arrows) of 8-week–old animals. In all relevant panels DAPI counterstaining is shown in blue.

During 45 h of EEG recording from 6 hypomorphic mice, clear electrographic seizures were observed in 3 animals (Fig. 7*D*). However, all hypomorphic mice displayed interictal spikes (not shown). During the recording period, only one of the electrographic seizures was associated with a stage 4 behavioral seizure, suggesting that the majority of the electrographically recorded seizures were restricted to the hippocampus. Normal activity was detected during 48 h of EEG recording from 6 control littermates (Fig. 7*C*). These studies demonstrate that reduced activity of *Lhx6* results in increased susceptibility to convulsive stimuli and development of spontaneous tonic-clonic and electrographic seizures.

In Lhx6 Hypomorphic Mice Histopathological Evidence of Seizures Develops After 4 Weeks of Age

To establish the onset of seizure activity in *Lhx6* hypomorphic animals, we determined the stage at which histological correlates of brain hyperexcitability emerge. Up-regulation of NPY is a well-established indicator of spontaneous or induced cortical hyperexcitability in rodents and is particularly evident in mossy fibers emanating from granule cells of the DG (Chafetz et al. 1995; Vezzani et al. 1999; Borges et al. 2003; Cobos et al. 2005). Strong NPY staining was observed in mossy fibers of most *Lhx6* hypomorphic animals (84%, $n = 19$) older than 8 weeks of age (Fig. 7*F*) but was absent from all similar age controls ($n = 9$; not shown). In contrast to these observations, 88% ($n = 8$) of 4-week–old hypomorphic and control mice lacked mossy fiber-specific NPY staining (Fig. 7*E* and data not shown). Seizures have also been associated with increased neurogenesis in the DG (Parent 2007). Therefore, we measured the incorporation of the nucleotide analog EdU (Fig. 7*G–J*) in the inner granular layer of the DG. Although at 4 weeks of age, EdU incorporation was similar between hypomorphic and control animals (Fig. 7*G,H,K*), at 8 weeks the number of EdU^+ cells was significantly higher in the DG of hypomorphic mice relative to controls (Fig. 7*I,J,L*). Consistent with enhanced neurogenesis, we also observed a marked increase in Cr immunostaining (a characteristic feature of newly born granule cells; Brandt et al. 2003) in the granule cell layer of 8-week–old hypomorphic mice when compared with 8-week–old controls or 4-week–old animals of either genotype (Fig. 7*M,N* and data not shown). We conclude that histopathological correlates of seizure activity appear between 4 and 8 weeks of age and are evident in the hippocampus of most *Lhx6* hypomorphic animals.

The Deficit of Sst^+ Cortical Interneuron Differentiation in Lhx6 Hypomorphic Mice Precedes the Onset of Tonic-Clonic Seizures

Seizure activity has been associated with a reduced number of Sst^+ interneurons in humans and in animal models of epilepsy. To examine whether the reduced number of Sst^+ interneurons observed in Lhx6 hypomorphic mice is secondary to the seizure activity in these animals, we determined the developmental stage at which the reduced expression of Sst first becomes apparent. Our analysis shows that the relative density of Sst^+ cells in hypomorphic mice was already reduced at E13.5 (Fig. 8*A,B,G*), was further decreased at E17.5 (Fig. 8*C,D,G*) and reached its lowest levels at P8 (density of Sst^+ cells at this stage in $Lhx6^{LacZ/-}$ cortex was 51 ± 4% of controls; $P = 0.002$; Fig. 8*E–G*). Consistent with our analysis of 4-week–old animals (Fig. 4), the residual population of Sst^+ interneurons in the cortex of P8 hypomorphic mice was mostly concentrated in the deep layers (Fig. 8*E,F*). Based on these findings, we suggest that defective differentiation of interneurons in the cortex of *Lhx6* hypomorphs, as highlighted by reduced expression of Sst, precedes the onset of seizure activity in these mice.

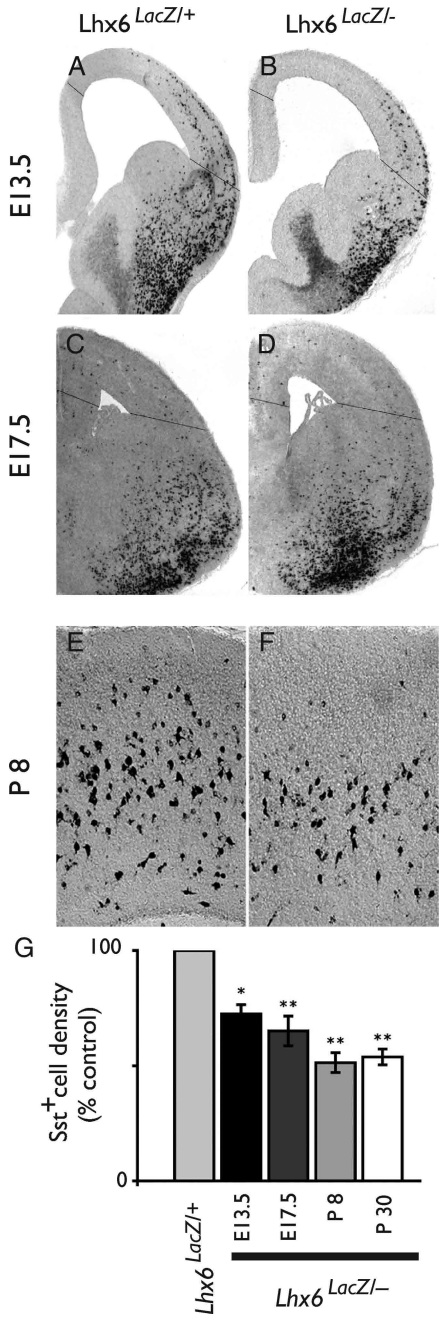

Figure 8. The deficit of Sst^+ neurons in the cortex of $Lhx6^{LacZ/-}$ animals is already present at embryonic stages. (*A–F*) *In situ* hybridization of brain sections from E13.5 (*A* and *B*), E17.5 (*C* and *D*), P8 (*E* and *F*), control ($Lhx6^{LacZ/+}$; *A*, *C*, *E*), and $Lhx6^{LacZ/-}$ (*B*, *D*, *F*) animals using an Sst-specific riboprobe. (*G*) Quantification of the average density of Sst^+ cells in the pallium (area between the lines in *A–D*) or the somatosensory cortex (for P8 and P30) in $Lhx6^{LacZ/-}$ animals relative to their control ($Lhx6^{LacZ/+}$) counterparts (*$P < 0.05$ and **$P < 0.01$; $n = 3$ animals per genotype and developmental stage).

Discussion

Lhx6 Plays a Role in Late Cortical Interneuron Differentiation

We and others have previously demonstrated that deletion of the LIM HD-encoding gene *Lhx6* results in defective tangential migration, abnormal distribution in the cortex, and failure of differentiation of Sst^+ and Pva^+ cortical interneurons (Liodis et al. 2007; Zhao et al. 2008). Here, we provide electrophysiological evidence that in the absence of Lhx6, the inhibitory input onto DG granule cells is dramatically reduced. These findings extend previous developmental studies and demonstrate that Lhx6 is required for the functional integration of cortical interneurons into the neuronal circuitry of the cerebral cortex. The striking deficit in inhibitory synaptic function observed in *Lhx6* null mutants could be secondary to the migratory defect associated with deletion of *Lhx6*, as failure of interneuron precursors to reach their final destination on time could prevent them from establishing functional connections with their post-synaptic targets. This view is consistent with the observation that rescue of the migratory deficit by the $Lhx6^{LacZ}$ allele results in normal perisomatic inhibition of dentate granule cells. However, despite normal tangential migration, density and distribution of interneurons in the cortical layers of *Lhx6* hypomorphic mice, these animals are characterized by widespread deficits in the differentiation of Sst^+ interneurons and altered physiology of inhibitory synapses at distal dendrites, which was associated with the development of spontaneous generalized tonic-clonic seizures. These results provide evidence for a cell-intrinsic role of *Lhx6* in cortical interneuron differentiation and identify a specific requirement for dendritic inhibition. Together with previous reports (Alifragis et al. 2004; Liodis et al. 2007; Zhao et al. 2008), our current findings suggest that Lhx6 controls multiple stages of cortical interneuron development, from specification and differentiation of MGE-derived interneuron precursors into distinct subtypes (highlighted by the early reduction of Sst expression in null and hypomorphic mutants), tangential migration and allocation to cortical layers, to maturation within the cortical plate and integration into inhibitory circuits. Characterization of mutants with subtype- and stage-specific deletion of *Lhx6* will provide critical insight into the different roles of *Lhx6* and its downstream effectors.

Reduced Lhx6 Activity Preferentially Affects Sst^+ Interneuron Differentiation

The molecular mechanisms that regulate the choice of MGE-progenitors to differentiate into Pva- or Sst-expressing interneurons are currently unclear. Recent studies suggest that the dorsal MGE, which co-expresses the HD transcription factors Nkx2.1 and Nkx6.2, gives rise preferentially to Sst^+ interneurons (Flames et al. 2007; Fogarty et al. 2007; Wonders et al. 2008; Sousa et al. 2009) and that high levels of sonic hedgehog (Shh) signaling promote the Sst fate (Xu, Guo et al. 2010). In contrast, BMP4 signaling and the activity of the transcriptional regulator Sox6 have been associated with Pva^+ interneuron differentiation (Batista-Brito et al. 2009; Mukhopadhyay et al. 2009). *Lhx6* hypomorphic mice have widespread deficits in the differentiation of Sst^+ interneurons, while Pva^+ interneuron differentiation defects were restricted to the DG of the hippocampus. These observations suggest a dose-dependent requirement of Lhx6 for the differentiation of Sst^+ and Pva^+ cortical interneurons and provide independent genetic evidence that distinct molecular mechanisms regulate the differentiation of cortical interneuron subclasses. Interestingly, Sst^+ interneurons that occupy the superficial cortical layers were preferentially affected in *Lhx6* hypomorphs. Since this subpopulation of interneurons are born during later stages of embryogenesis (Valcanis and Tan 2003), our findings also suggest a stage-dependent requirement of *Lhx6* activity. Understanding further the dose- and stage-dependent roles of Lhx6 in interneuron development should provide critical insight into the molecular mechanisms that underlie the formation of functional inhibitory circuits by cortical interneurons.

Defects in Sst^+ Interneuron Differentiation are Likely to Lead to Selective Alterations in the Function of Dendritic Synapses

Pva^+ interneurons (such as basket or Chandelier cells) form synapses preferentially onto the soma and axonal initial segment of their target cells, whereas Sst^+ interneurons (such as OLM or Martinotti cells) target mostly distal dendrites (Miles et al. 1996; Kawaguchi and Kubota 1997; Maccaferri et al. 2000; Wang et al. 2004; Butt et al. 2005). Several lines of evidence suggest that inhibitory synapses at different cellular compartments have distinct functional properties, which are likely to reflect their unique molecular features. For example, GABA-A receptors at perisomatic synapses formed by Pva^+ interneurons in the hippocampus contain mainly alpha1 subunits (Nusser et al. 1996), while synapses at distal dendrites forming by Sst^+ interneurons contain alpha5 subunits (Serwanski et al. 2006; Ali and Thomson 2008). Consistent with the normal differentiation of Pva^+ interneurons in the CA1 region of the hippocampus of *Lhx6* hypomorphic mice, the physiological properties of IPSCs recorded from the soma of pyramidal cells were indistinguishable to those observed in control animals. In contrast, dendritic mIPSCs from the same hippocampal region showed characteristic changes in the frequency and kinetics, suggesting changes in the properties of both pre- and post-synaptic compartments of inhibitory synapses. We suggest that the changes of these parameters in *Lhx6* hypomorphic mice constitute physiological correlates of the differentiation defects of Sst^+ interneurons observed in these animals. Alternatively, the increased frequency of mIPSCs in the dendrites may represent a homeostatic response to compensate for the increased excitability of the hippocampal network. Although the mechanisms underlying the observed changes in the physiology of dendritic synapses are currently unclear, our experiments argue that reduced *Lhx6* activity directly controls multiple aspects of the differentiation and synaptic connectivity of Sst^+ cortical interneurons.

Lhx6 Hypomorphic Mutants as a New Mouse Model of Epileptogenesis

Several animal models with mutations in transcription factor-encoding genes that control different aspects of cortical interneuron development are characterized by defects in inhibitory circuits and epilepsy. Thus, deletion of *Dlx1*, *Nkx2.1*, *Arx*, and *Sox6* results in the appearance of spontaneous seizures (Kitamura et al. 2002; Cobos et al. 2005; Butt et al. 2008;

Batista-Brito et al. 2009). The severe deficit of inhibitory synapses observed in the cortex of *Lhx6* null mutants suggests that these animals are likely to develop seizures, although the early post-natal lethality and weakness of these animals preclude their systematic analysis. The presence of seizure activity in *Lhx6* null mutants is suggested by the up-regulation of activity-dependent genes, such as c-fos, Arc, NPY, and BDNF in 2-week–old animals (unpublished observations). Moreover, direct demonstration that the absence of *Lhx6* activity results in the development of tonic-clonic seizures has been achieved in animals in which *Lhx6* was specifically ablated in MGE-derived cortical interneurons (M Kalaitzidou, G.N. and V.P., unpublished observations).

Consistent with these findings, the reduced activity of *Lhx6* observed in $Lhx6^{LacZ}$ hypomorphic leads to adult onset epilepsy, which is likely to represent the mild end of the spectrum of epileptic phenotypes observed in *Lhx6* mutants. Null mutations in *Dlx1* also result in adult onset epilepsy, which are characterized by cell death of a subset of Sst-, Cr-, and NPY-expressing interneurons and reduced inhibitory synaptic function (Cobos et al. 2005). In contrast, the adult onset epilepsy observed in *Lhx6* hypomorphic mice is not associated with either cell death or reduced inhibition. Instead, these animals are characterized by an early specific deficit in the differentiation of the Sst-expressing interneurons, which are likely to be implicated in the pathophysiological mechanisms of epileptogenesis. We propose that the profound loss of mGluR1α expression in *stratum oriens* in *Lhx6* hypomorphs leads to decreased efficiency of the recurrent inhibition provided by Sst^+ OLM cells (Andersen et al. 1963; Freund and Buzsaki 1996). mGluR1α is necessary for long term potentiation induction in OLM interneurons (Lapointe et al. 2004), and mGluR1α activation leads to an increased frequency of spontaneous IPSCs in CA1 pyramidal cells (Mannaioni et al. 2001). This model is consistent with our observations that no changes were observed in the dendritic sIPSC frequency in *Lhx6* hypomorphic mice, despite the increased frequency of dendritic mIPSCs. It is important to note, however, that the decrease in the expression of Pva in the DG region of the hippocampus we observed might also have an impact on epileptogenesis. Further studies on this mouse model will provide insight into the molecular and physiological mechanisms regulating interneuron differentiation and epileptogenesis.

Supplementary Material

Supplementary material can be found at: http://www.cercor.oxfordjournals.org/.

Funding

This work was supported by a Medical Research Council (MRC) Grant-in-Aid to V.P. (U117537087) and an MRC grant to M.S. (G0700369). Funding to pay the Open Access publication charges for this article was provided by the Medical Research Council.

Notes

We thank Martyn Stopps and the Mechanical Engineering Division (NIMR) for help with setting up the electrophysiological recordings and the video monitoring of behavior; Karri Lamsa (University of Oxford) for advice with the preparation of mouse hippocampal slices; Diogo Castro and Ben Martynoga (Molecular Neurobiology, NIMR) for help with setting up real-time polymerase chain reaction experiments and the Biological Services Division (NIMR) for animal husbandry. *Conflict of Interest*: None declared.

References

Ali AB, Thomson AM. 2008. Synaptic alpha 5 subunit-containing GABAA receptors mediate IPSPs elicited by dendrite-preferring cells in rat neocortex. Cereb Cortex. 18:1260–1271.

Alifragis P, Liapi A, Parnavelas JG. 2004. Lhx6 regulates the migration of cortical interneurons from the ventral telencephalon but does not specify their GABA phenotype. J Neurosci. 24:5643–5648.

Andersen P, Eccles JC, Loyning Y. 1963. Recurrent inhibition in the hippocampus with identification of the inhibitory cell and its synapses. Nature. 198:540–542.

Andrasfalvy BK, Mody I. 2006. Differences between the scaling of miniature IPSCs and EPSCs recorded in the dendrites of CA1 mouse pyramidal neurons. J Physiol. 576:191–196.

Ascoli GA, Alonso-Nanclares L, Anderson SA, Barrionuevo G, Benavides-Piccione R, Burkhalter A, Buzsaki G, Cauli B, Defelipe J, Fairen A *et al.*. 2008. Petilla terminology: nomenclature of features of GABAergic interneurons of the cerebral cortex. Nat Rev Neurosci. 9:557–568.

Batista-Brito R, Rossignol E, Hjerling-Leffler J, Denaxa M, Wegner M, Lefebvre V, Pachnis V, Fishell G. 2009. The cell-intrinsic requirement of Sox6 for cortical interneuron development. Neuron. 63:466–481.

Baude A, Nusser Z, Roberts JD, Mulvihill E, McIlhinney RA, Somogyi P. 1993. The metabotropic glutamate receptor (mGluR1 alpha) is concentrated at perisynaptic membrane of neuronal subpopulations as detected by immunogold reaction. Neuron. 11:771–787.

Borges K, Gearing M, McDermott DL, Smith AB, Almonte AG, Wainer BH, Dingledine R. 2003. Neuronal and glial pathological changes during epileptogenesis in the mouse pilocarpine model. Exp Neurol. 182:21–34.

Brandt MD, Jessberger S, Steiner B, Kronenberg G, Reuter K, Bick-Sander A, von der Behrens W, Kempermann G. 2003. Transient calretinin expression defines early postmitotic step of neuronal differentiation in adult hippocampal neurogenesis of mice. Mol Cell Neurosci. 24:603–613.

Butt SJ, Fuccillo M, Nery S, Noctor S, Kriegstein A, Corbin JG, Fishell G. 2005. The temporal and spatial origins of cortical interneurons predict their physiological subtype. Neuron. 48:591–604.

Butt SJ, Sousa VH, Fuccillo MV, Hjerling-Leffler J, Miyoshi G, Kimura S, Fishell G. 2008. The requirement of Nkx2-1 in the temporal specification of cortical interneuron subtypes. Neuron. 59:722–732.

Chafetz RS, Nahm WK, Noebels JL. 1995. Aberrant expression of neuropeptide Y in hippocampal mossy fibers in the absence of local cell injury following the onset of spike-wave synchronization. Brain Res Mol Brain Res. 31:111–121.

Cobos I, Calcagnotto ME, Vilaythong AJ, Thwin MT, Noebels JL, Baraban SC, Rubenstein JL. 2005. Mice lacking Dlx1 show subtype-specific loss of interneurons, reduced inhibition and epilepsy. Nat Neurosci. 8:1059–1068.

de Curtis M, Gnatkovsky V. 2009. Reevaluating the mechanisms of focal ictogenesis: the role of low-voltage fast activity. Epilepsia. 50:2514–2525.

Du T, Xu Q, Ocbina PJ, Anderson SA. 2008. NKX2.1 specifies cortical interneuron fate by activating Lhx6. Development. 135:1559–1567.

Ferraguti F, Cobden P, Pollard M, Cope D, Shigemoto R, Watanabe M, Somogyi P. 2004. Immunolocalization of metabotropic glutamate receptor 1alpha (mGluR1alpha) in distinct classes of interneuron in the CA1 region of the rat hippocampus. Hippocampus. 14:193–215.

Flames N, Pla R, Gelman DM, Rubenstein JL, Puelles L, Marin O. 2007. Delineation of multiple subpallial progenitor domains by the combinatorial expression of transcriptional codes. J Neurosci. 27:9682–9695.

Fogarty M, Grist M, Gelman D, Marin O, Pachnis V, Kessaris N. 2007. Spatial genetic patterning of the embryonic neuroepithelium generates GABAergic interneuron diversity in the adult cortex. J Neurosci. 27:10935–10946.
Freund TF, Buzsaki G. 1996. Interneurons of the hippocampus. Hippocampus. 6:347–470.
Fu LY, van den Pol AN. 2007. GABA excitation in mouse hilar neuropeptide Y neurons. J Physiol. 579:445–464.
Huang Z, Walker MC, Shah MM. 2009. Loss of dendritic HCN1 subunits enhances cortical excitability and epileptogenesis. J Neurosci. 29:10979–10988.
Kawaguchi Y, Kubota Y. 1997. GABAergic cell subtypes and their synaptic connections in rat frontal cortex. Cereb Cortex. 7:476–486.
Kitamura K, Yanazawa M, Sugiyama N, Miura H, Iizuka-Kogo A, Kusaka M, Omichi K, Suzuki R, Kato-Fukui Y, Kamiirisa K *et al.*. 2002. Mutation of ARX causes abnormal development of forebrain and testes in mice and X-linked lissencephaly with abnormal genitalia in humans. Nat Genet. 32:359–369.
Lapointe V, Morin F, Ratte S, Croce A, Conquet F, Lacaille JC. 2004. Synapse-specific mGluR1-dependent long-term potentiation in interneurones regulates mouse hippocampal inhibition. J Physiol. 555:125–135.
Lavdas AA, Grigoriou M, Pachnis V, Parnavelas JG. 1999. The medial ganglionic eminence gives rise to a population of early neurons in the developing cerebral cortex. J Neurosci. 19:7881–7888.
Liodis P, Denaxa M, Grigoriou M, Akufo-Addo C, Yanagawa Y, Pachnis V. 2007. Lhx6 activity is required for the normal migration and specification of cortical interneuron subtypes. J Neurosci. 27:3078–3089.
Maccaferri G, Roberts JD, Szucs P, Cottingham CA, Somogyi P. 2000. Cell surface domain specific postsynaptic currents evoked by identified GABAergic neurones in rat hippocampus in vitro. J Physiol. 524(Pt 1):91–116.
Mannaioni G, Marino MJ, Valenti O, Traynelis SF, Conn PJ. 2001. Metabotropic glutamate receptors 1 and 5 differentially regulate CA1 pyramidal cell function. J Neurosci. 21:5925–5934.
Miles R, Toth K, Gulyas AI, Hajos N, Freund TF. 1996. Differences between somatic and dendritic inhibition in the hippocampus. Neuron. 16:815–823.
Monory K, Massa F, Egertova M, Eder M, Blaudzun H, Westenbroek R, Kelsch W, Jacob W, Marsch R, Ekker M *et al.*. 2006. The endocannabinoid system controls key epileptogenic circuits in the hippocampus. Neuron. 51:455–466.
Mukhopadhyay A, McGuire T, Peng CY, Kessler JA. 2009. Differential effects of BMP signaling on parvalbumin and somatostatin interneuron differentiation. Development. 136:2633–2642.
Nusser Z, Sieghart W, Benke D, Fritschy JM, Somogyi P. 1996. Differential synaptic localization of two major gamma-aminobutyric acid type A receptor alpha subunits on hippocampal pyramidal cells. Proc Natl Acad Sci USA. 93:11939–11944.
Oren I, Nissen W, Kullmann DM, Somogyi P, Lamsa KP. 2009. Role of ionotropic glutamate receptors in long-term potentiation in rat hippocampal CA1 oriens-lacunosum moleculare interneurons. J Neurosci. 29:939–950.
Parent JM. 2007. Adult neurogenesis in the intact and epileptic dentate gyrus. Prog Brain Res. 163:529–540.
Paxinos G, Franklin K. 2001. The mouse brain in stereotaxic coordinates. New York: Academic Press.
Rossignol E. 2011. Genetics and function of neocortical GABAergic interneurons in neurodevelopmental disorders. Neural Plast. 2011:649325.
Rubenstein JL. 2011. Annual research review: development of the cerebral cortex: implications for neurodevelopmental disorders. J Child Psychol Psychiatry. 52:339–355.
Rudy B, Fishell G, Lee S, Hjerling-Leffler J. 2011. Three groups of interneurons account for nearly 100% of neocortical GABAergic neurons. Dev Neurobiol. 71:45–61.
Schaeren-Wiemers N, Gerfin-Moser A. 1993. A single protocol to detect transcripts of various types and expression levels in neural tissue and cultured cells: in situ hybridization using digoxigenin-labelled cRNA probes. Histochemistry. 100:431–440.
Segev I, Rall W. 1998. Excitable dendrites and spines: earlier theoretical insights elucidate recent direct observations. Trends Neurosci. 21:453–460.
Serwanski DR, Miralles CP, Christie SB, Mehta AK, Li X, De Blas AL. 2006. Synaptic and nonsynaptic localization of GABAA receptors containing the alpha5 subunit in the rat brain. J Comp Neurol. 499:458–470.
Somogyi P, Klausberger T. 2005. Defined types of cortical interneurone structure space and spike timing in the hippocampus. J Physiol. 562:9–26.
Sousa VH, Miyoshi G, Hjerling-Leffler J, Karayannis T, Fishell G. 2009. Characterization of Nkx6-2-derived neocortical interneuron lineages. Cereb Cortex. 19(Suppl 1):i1–i10.
Sussel L, Marin O, Kimura S, Rubenstein JL. 1999. Loss of Nkx2.1 homeobox gene function results in a ventral to dorsal molecular respecification within the basal telencephalon: evidence for a transformation of the pallidum into the striatum. Development. 126:3359–3370.
Valcanis H, Tan SS. 2003. Layer specification of transplanted interneurons in developing mouse neocortex. J Neurosci. 23:5113–5122.
Vezzani A, Sperk G, Colmers WF. 1999. Neuropeptide Y: emerging evidence for a functional role in seizure modulation. Trends Neurosci. 22:25–30.
Wang Y, Toledo-Rodriguez M, Gupta A, Wu C, Silberberg G, Luo J, Markram H. 2004. Anatomical, physiological and molecular properties of Martinotti cells in the somatosensory cortex of the juvenile rat. J Physiol. 561:65–90.
Welagen J, Anderson S. 2011. Origins of neocortical interneurons in mice. Dev Neurobiol. 71:10–17.
Williams SR, Mitchell SJ. 2008. Direct measurement of somatic voltage clamp errors in central neurons. Nat Neurosci. 11:790–798.
Wonders CP, Anderson SA. 2006. The origin and specification of cortical interneurons. Nat Rev Neurosci. 7:687–696.
Wonders CP, Taylor L, Welagen J, Mbata IC, Xiang JZ, Anderson SA. 2008. A spatial bias for the origins of interneuron subgroups within the medial ganglionic eminence. Dev Biol. 314:127–136.
Xu Q, Cobos I, De La Cruz E, Rubenstein JL, Anderson SA. 2004. Origins of cortical interneuron subtypes. J Neurosci. 24:2612–2622.
Xu Q, Guo L, Moore H, Waclaw RR, Campbell K, Anderson SA. 2010. Sonic hedgehog signaling confers ventral telencephalic progenitors with distinct cortical interneuron fates. Neuron. 65:328–340.
Xu X, Roby KD, Callaway EM. 2010. Immunochemical characterization of inhibitory mouse cortical neurons: three chemically distinct classes of inhibitory cells. J Comp Neurol. 518:389–404.
Xu X, Roby KD, Callaway EM. 2006. Mouse cortical inhibitory neuron type that coexpresses somatostatin and calretinin. J Comp Neurol. 499:144–160.
Zhao Y, Flandin P, Long JE, Cuesta MD, Westphal H, Rubenstein JL. 2008. Distinct molecular pathways for development of telencephalic interneuron subtypes revealed through analysis of Lhx6 mutants. J Comp Neurol. 510:79–99.